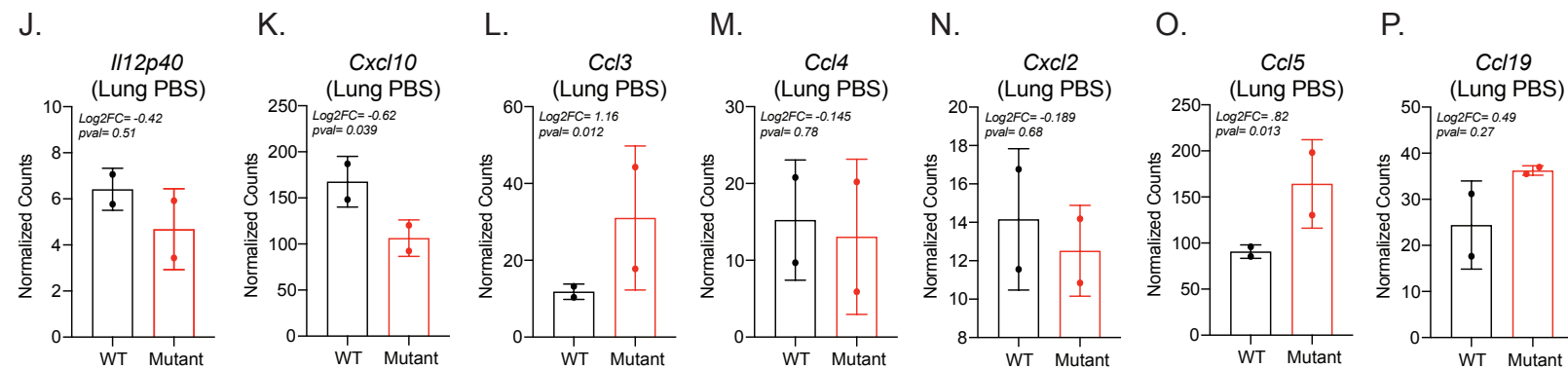
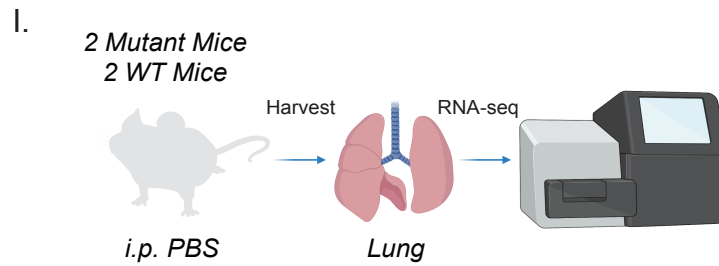
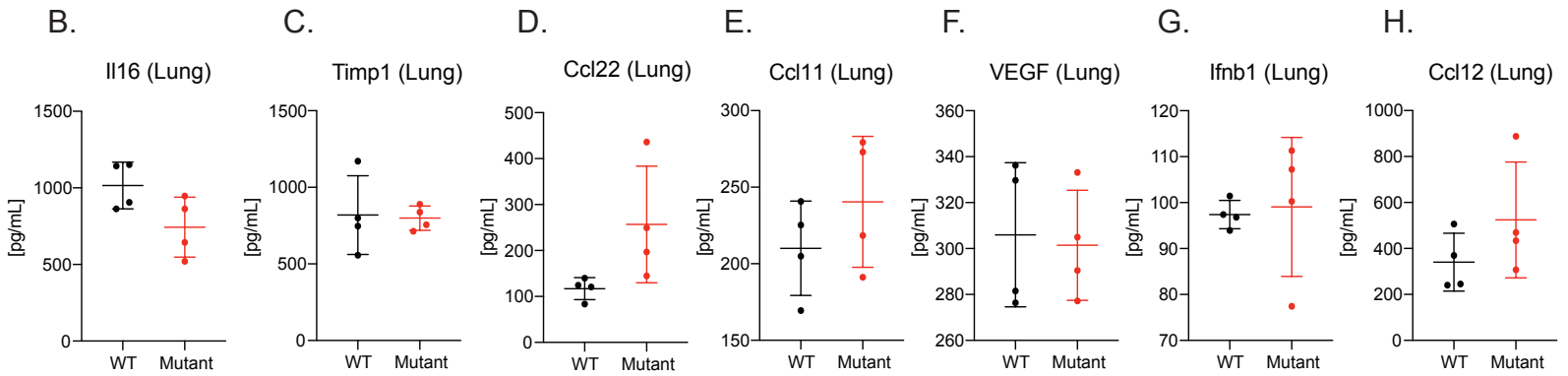
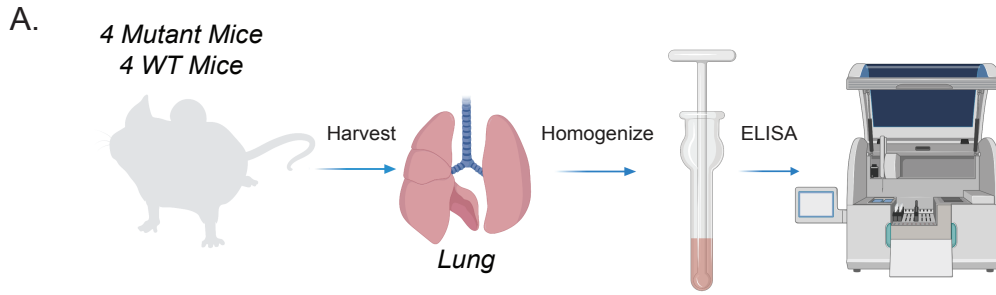


Supplemental Figure 1

	Knockout Mouse	Mutant Mouse	Transgenic Mouse
Mouse Design			
Technology	VelociGene technology	CRISPR/Cas9	Site-specific TARGATT
<i>lincRNA-Cox2</i> Expression	not expressed	expressed at baseline, not inducible	expressed at the level of house-keeping genes
Ptgs2 Expression	heavily downregulated, no protein expression	not effected, same as WT	not effected, same as WT
<i>lincRNA-Cox2</i> mechanism	<i>cis</i> and <i>trans</i>	<i>trans</i>	<i>trans</i>

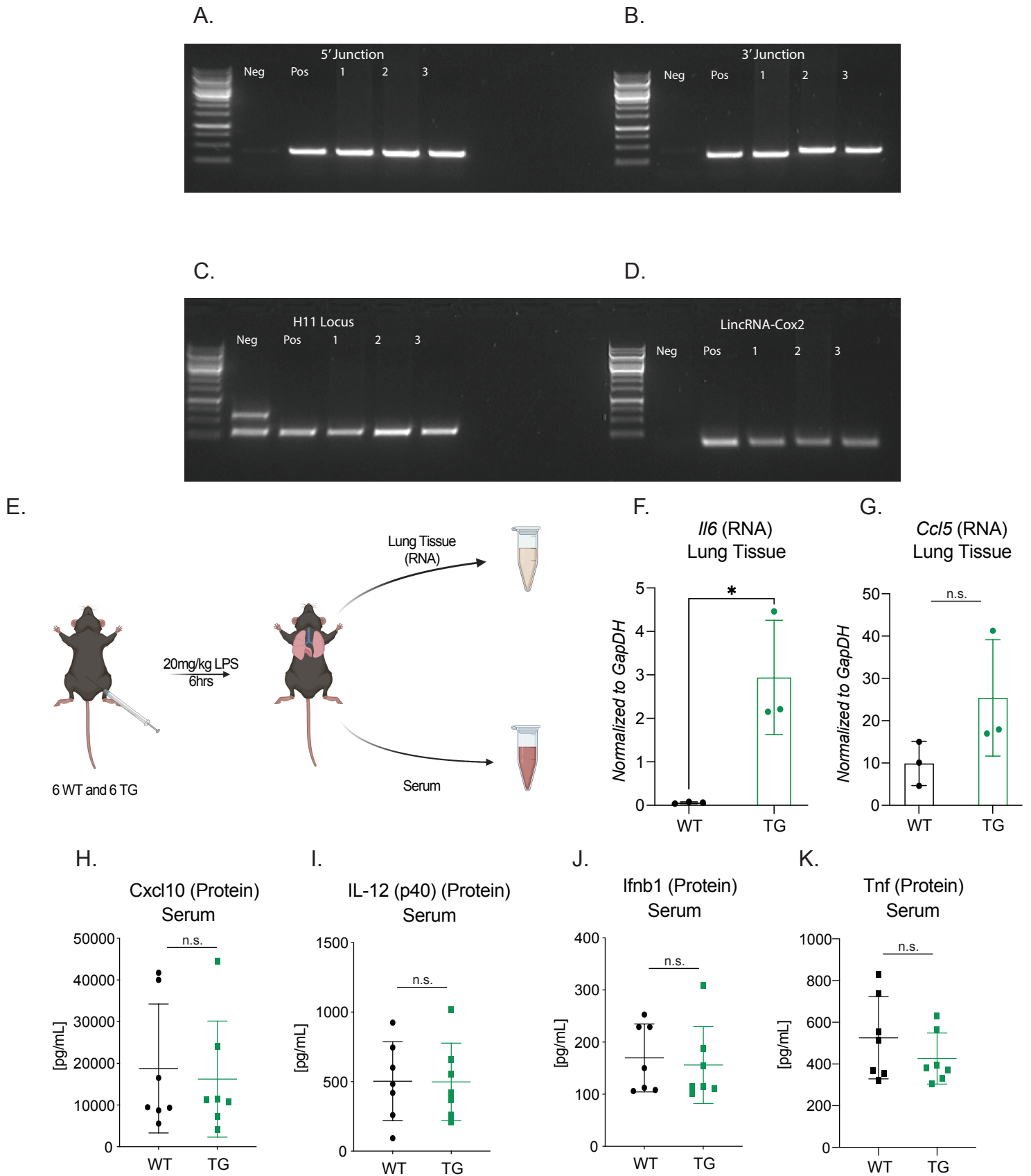
Supplemental Figure 1: Chart of defining all *lincRNA-Cox2* mice models. To understand the different mouse models the chart includes: how the mice were designed, the technology used to generate the mice, the expression of *lincRNA-Cox2* and Ptgs2, as well as the mechanism.

Supplemental Figure 2



Supplemental Figure 2: Characterization of immune pathways in *lincRNA-Cox2* mutant at baseline. (A) Schematic of cytokine analysis of lung homogenates from WT and mutant mice. Multiplex cytokine analysis was performed on lung homogenates for (B) Il16, (C) Timp1, (D) Ccl22, (E) Ccl11, (F) Vegf, (G) Ifnb1 and (H) Ccl12. (I) Schematic of RNA-seq analysis of WT and Mutant lungs at baseline. Normalized counts for (J) Il12p40, (K) Cxcl10, (L) Ccl3, (M) Ccl4, (N) Cxcl2, (O) Ccl5 and (P) Ccl19. Student's t-test used to determine significance and asterisks indicate statistical significance (*=> 0.05, **=>.01, ***=> 0.0005).

Supplemental Figure 3

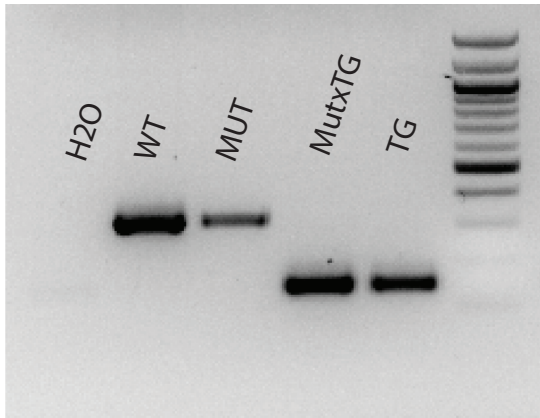


Supplemental Figure 3: PCR strategy and further characterization of transgenic *lincRNA-Cox2* mouse using the TARGATT system. Generation of transgenic mouse with the TARGATT system. This process allowed recombination at the H11 locus. Specific primer sets were used to confirm correct integration of *lincRNA-Cox2*. The strategy used to generate the *lincRNA-Cox2* transgenic mice was adapted from Tasica et al, PNAS 2011 and genotyping (A-D) strategy was utilized to confirm homozygosity. (E) Schematic of WT and Transgenic septic shock model. RNA was isolated from lung tissue to measure mRNA expression of (F) *Il6* and (G) *Ccl5*, normalized to *GapDH*. Serum was harvested to measure (H) *Cxcl10*, (I) *Il12*p40, (J) *Il1b* and (K) *Tnf* by ELISA. Student's t-test used to determine significance and asterisks indicate statistical significance (*=> 0.05, **=>.01, ***=> 0.0005).

Supplemental Figure 4

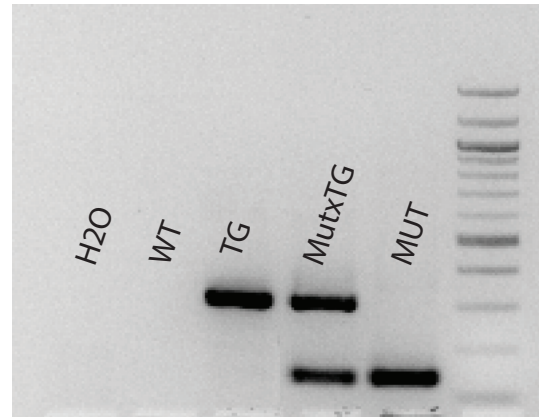
A.

PCR7/8 TARGATT Primers



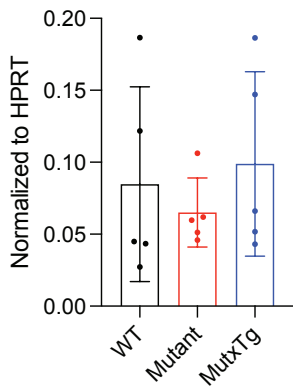
B.

lincRNA-Cox2 F/R Primers



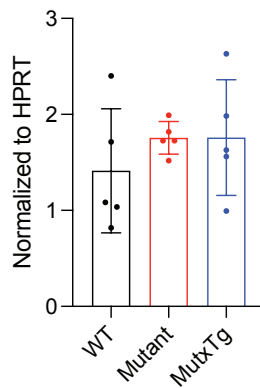
C.

IL6 (mRNA)



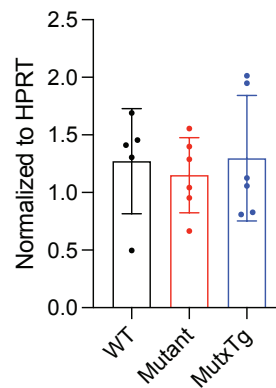
D.

Ccl5 (mRNA)



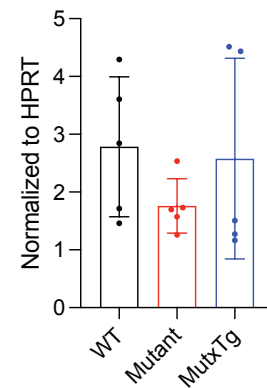
E.

Ccl3 (mRNA)



F.

Ccl4 (mRNA)



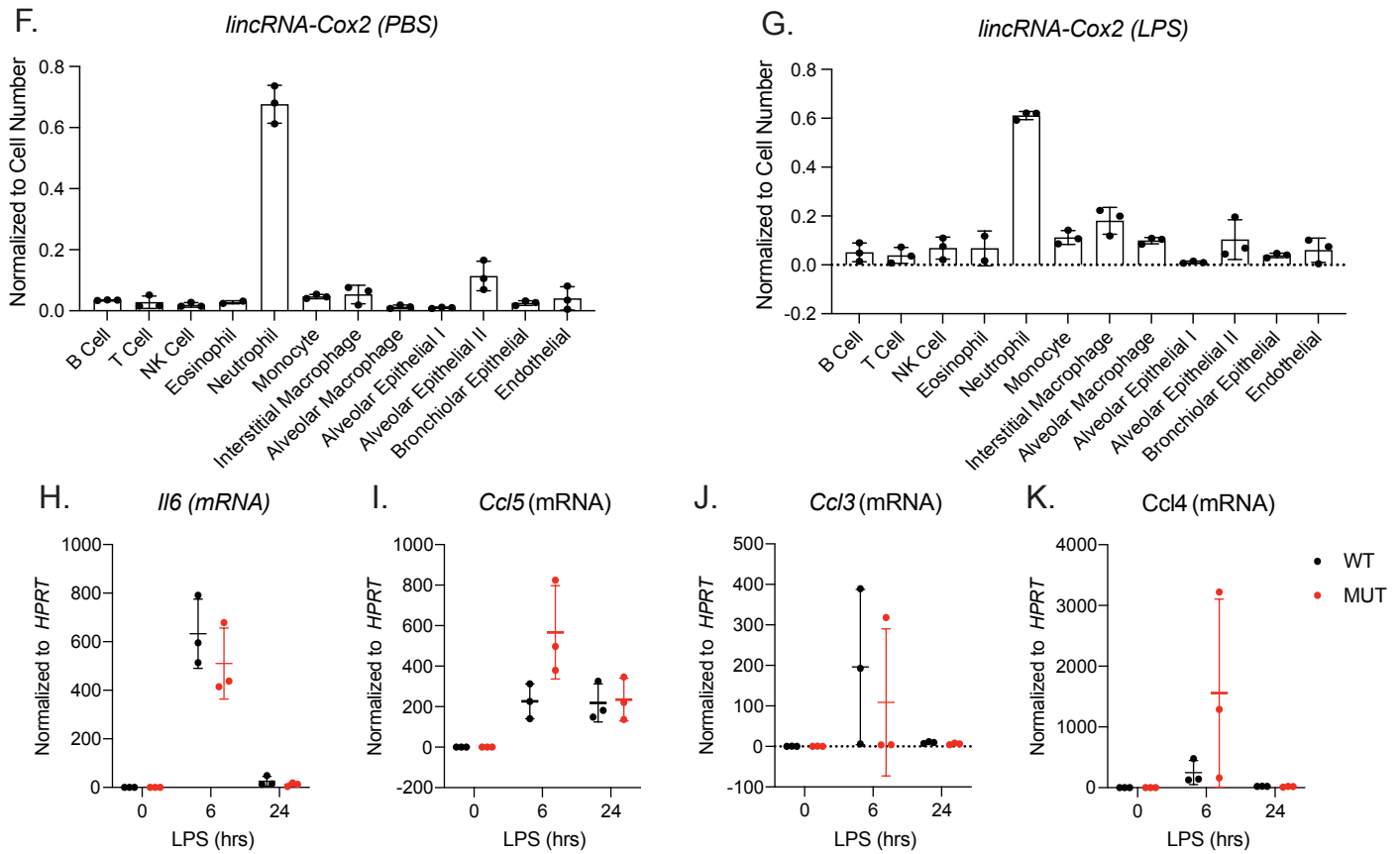
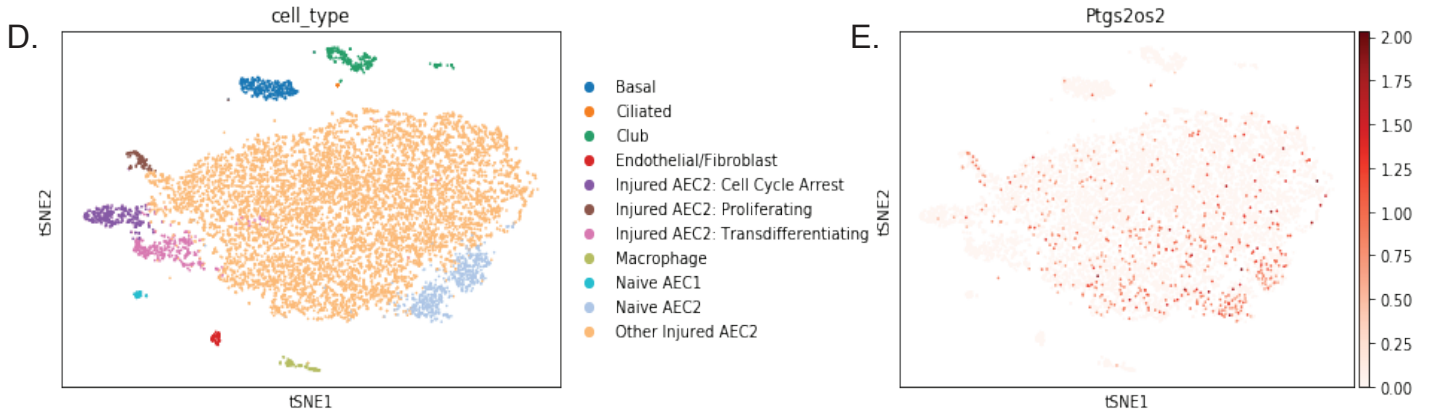
Supplemental Figure 4: Genotyping strategy and transcriptional regulation in BAL cells for MutxTG *lincRNA-Cox2* mouse. (A) PCR7/8 TARGATT primers were utilized to check for homozygosity. (B) *lincRNA-Cox2* specific primers were utilized to assess homozygosity of mutant mouse allele. *lincRNA-Cox2* RNA isolations were performed on BAL cells harvested from ALI treated WT, *lincRNA-Cox2* Mutant and *lincRNA-Cox2* MutxTg mice to measure mRNA expression of (C) *Il6*, (D) *Ccl5*, (E) *Ccl3* and (F) *Ccl4*.

Supplemental Figure 5

Single cell RNA sequencing of alveolar macrophage from mice following LPS-induced lung injury

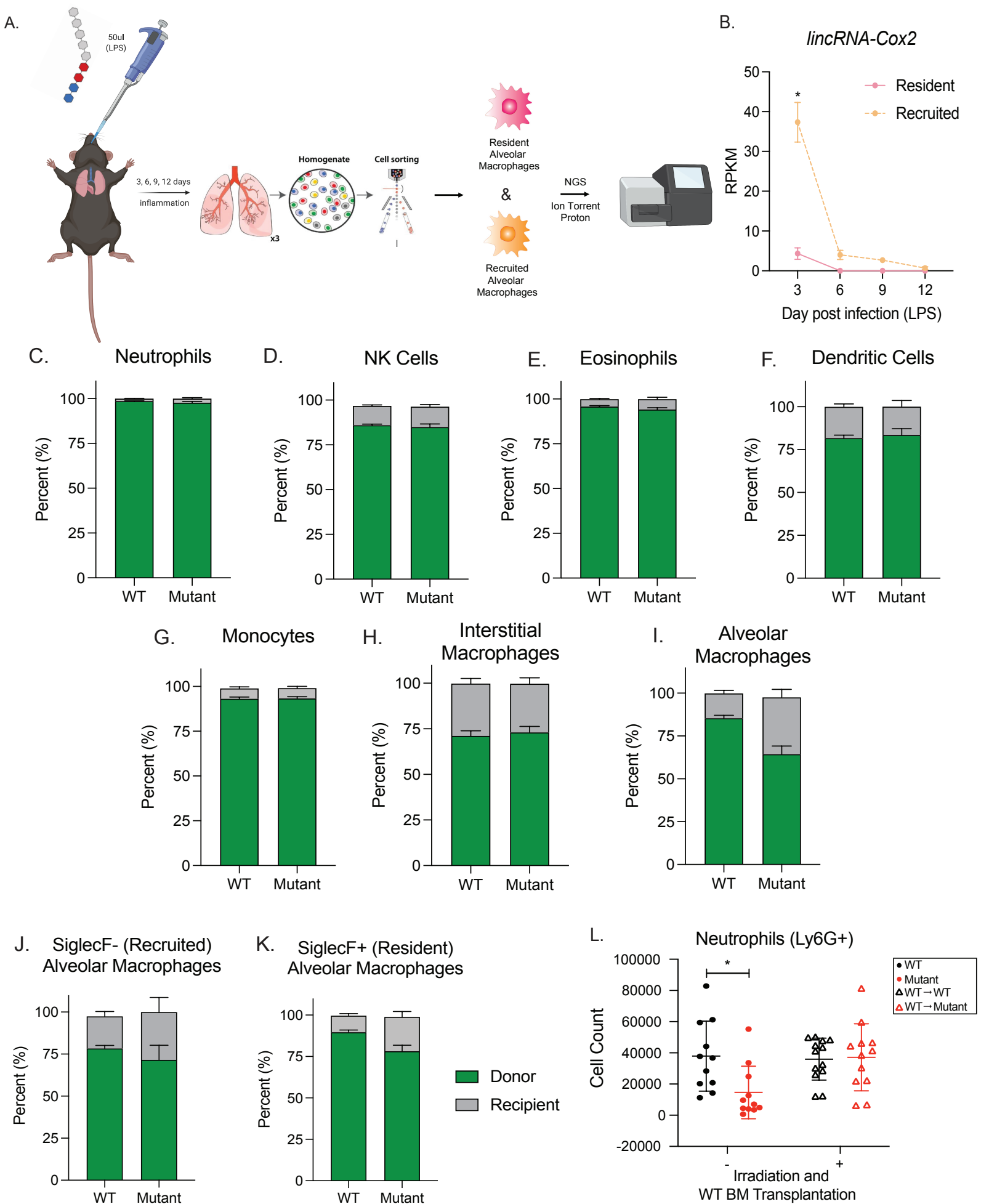


Single-cell RNA sequencing of CD45- cells from mice lung tissue following LPS-induced lung injury



Supplemental Figure 5: *lincRNA-Cox2* expression and transcriptional regulation in alveolar macrophages. Mould et al. generated scRNA-seq of alveolar macrophages from WT mice pre- and post- LPS induced acute lung injury. (A) tSNE plots were generated indicating 5 distinct populations. Then tSNE plots were utilized to examine (B) day of LPS stimulation and (C) *lincRNA-Cox2* (*ptgs2os2*) expression. Riemony et al. generated scRNA-seq of all CD45- cells from WT mice pre- and post- LPS induced acute lung injury. (D) tSNE plots were generated and clusters were colored based on cell type and (E) *lincRNA-Cox2* (*ptgs2os2*) expression. *lincRNA-Cox2* was measured in whole lung tissue and a number of sorted immune and epithelial cells from mice treated with (F) PBS and (G) LPS via an oropharyngeal route. Performed in biological triplicates and student's t-test was performed between whole lung tissue and each sorted cell. Primary alveolar macrophages were harvested, treated ex vivo with LPS for 0, 6h, and 24h. RNA was harvested, and RT-qPCR was used to measure mRNA expression of (H) *Il6*, (I) *Ccl5*, (J) *Ccl3* and (K) *Ccl4*.

Supplemental Figure 6



Supplemental Figure 6: *lincRNA-Cox2* functions within a bone marrow derived cell during ALI.

(A) Mould et al. generated bulk RNA-sequencing data of sorted resident and recruited alveolar macrophages. (B) *lincRNA-Cox2* was measured by normalized reads per kilobase of transcript (RPKM) in sorted recruited (pink) and resident (orange) alveolar macrophages. Donor (green) and recipient (grey) percentage were assessed for (C) Neutrophils, (D) NK cells, (E) Eosinophils, (F) Dendritic cells, (G) Monocytes, (H) Eosinophils, (I) Interstitial macrophages, (J) Alveolar macrophages, (K) Recruited alveolar macrophages and (L) Resident Alveolar macrophages. (L) Flow cytometry was utilized to assess raw cell counts of neutrophils from BAL cells of harvested from WT and *lincRNA-Cox2* mutant mice, as well as BMT WT→WT and WT→Mut during LPS induced ALI.

Supplemental Table 2: Antibodies used in flow cytometry experiments

Marker	Biologend	Fluorophore	Clone
Live/Dead	420404	7-AAD (695/40)	
Ly6G	127618	BV605	1A8
CD11c	117308	PE	N418
CD11b	101226	BV786	M1/70
IA/IE	107641	BV650	M5/114.15.2
CD64	139306	FITC	X54-5/7.1
CD24	101836	Alexa 700	M1/69
Ly6C	128014	PB	HK1.4
CD45	103140	BV510	30-F11
SiglecF	155504	APC	S17007L
CD90	140310	BV605	53-2.1
CD326	118233	BV711	G8.8
MHC-II I-A	116410	FITC	AF6-120.1
CD24	138504	Alexa 700	30-F1
T1a/Pdpn	127418	APC-Cy7	8.1.1
CD31	102410	APC	390
Ly6G	127612	PB	1A8
IA/IE	107628	APC-Cy7	M5/114.15.2
CD64	139314	PE-Cy7	X54-5/7.1
CD24	101827	BV605	M1/69
CD45	103128	A700	30-F11